P-ISSN 2586-9000
E-ISSN 2586-9027
Homepage : https://tci-thaijo.org/index.php/SciTechAsia
Science & Technology Asia
Vol.27 No.2 April - June 2022
Page: [148-170]
Original research article

Influence of Natural Rubber Latex on Carbonation of Calcined Clay-based Geopolymer Concrete

Badrinarayan Rath*

Department of Civil Engineering, Wollega University, Nekemte 395, Ethiopia

Received 16 December 2020; Received in revised form 25 March 2021
Accepted 19 April 2021; Available online 29 June 2022

ABSTRACT

Generally, the geopolymer concrete shows much less amount of workability as compared to traditional cement concrete of the same grade. People are using chemical superplasticizers on the higher side of the prescribed percentage range, to improve the workability of geopolymer concrete. But chemical superplasticizers, available in the local market are hazardous and highly expensive. Also, a high dose of chemical superplasticizer prolongs the setting time of concrete and cannot be remolded easily at the stipulated time. Poly Carboxylate Easter-based admixture creates bleeding initially and later makes the mix stick which creates a honeycomb. In this research, rubber latex was used as an admixture in cement concrete as well as calcined clay-based geopolymer concrete up to 2% of cementitious material, and carbonation depths were measured. Other tests, such as Ultrasonic Pulse Velocity (UPV), Bulk Electrical Resistivity (ER), TGA and tests for major constituents' solubility were conducted on various mixes of cement and geopolymer concrete. It was found that the higher dose of rubber latex provides a coating on cementitious material as well as the surface of the concrete structure. Hence, the resistance against diffusion of carbon dioxide gas comparatively increased when high dose rubber latex was used as an admixture. The carbonic service life periods for both cement and geopolymer concrete mixes were calculated and it was found that the carbonic service life period doubled when 2% of rubber latex was used as an admixture. A mathematical co-relation has been developed between UPV, ER and the diffusion coefficient of carbon dioxide.

Keywords: Brick aggregate; Calcined clay; Carbonation; Glass fiber; Geopolymer concrete; Rubber latex

***Corresponding author:** rath_rcpit@rediffmail.com **doi:** 10.14456/scitechasia.2022.32

1. Introduction

Concrete can be deteriorated due to three main reasons. They may be (i) physical or chemical deterioration of concrete itself, (ii) physical damage to concrete and (iii) corrosion of the reinforcement [1]. The main reasons for the corrosion of reinforcement in concrete are chloride attack and carbonation [2]. Carbonation is an important phenomenon for the durability of concrete structures in an atmospheric environment. The concentration of carbon dioxide beyond a certain limit accelerates the carbonation process in the Reinforced Cement Concrete (RCC) structure where steel becomes susceptible to corrosion. The carbonation process is considered as a deterioration mechanism in cementitious structures because it decreases the pH value of concrete [3]. On the other hand, carbonation is beneficial when there is no reinforcement in concrete mass. Because the end product of the carbonation reaction has a larger volume than the $Ca(OH)_2$, it fills the cement concrete pores by improving the microstructure and increasing its strength [4]. The carbon dioxide gas progressively changes the structure of C-S-H by removing Ca^{2+} ions and forming long silicate chain length [5]. In contrast, on exposure to accelerated carbonation the porosity of fly ash-based geopolymer concrete increases [6]. The pH value of concrete structures may change by gaining acid from the environment (i.e. carbon dioxide from the air and acid rain from the sky). The rate of corrosion depends upon the environmental condition, indirectly to the permeability of concrete to carbon dioxide and chloride. That means the environmental condition depends upon the amount of moisture in the cover zone, whereas moisture content depends upon the degree of saturation of concrete pores. The amount of unsaturated concrete pores increases the gas and liquid permeability which accelerates the corrosion process [7]. When the CO_2 reacts with dissolved minerals present in the cement pore water matrix alkalinity gets depleted and changes the solubility of pH-dependent constituents [8]. Also, the pore structure of the matrix is affected by the precipitation produced from carbonation reaction [9]. Finally, the carbonation leads to depassivation of reinforcing steel, degradation of concrete, and strength loss due to cracking in both nuclear and non-nuclear applications. Hence, a considerable effort should be focused on the primary degradation mechanisms of newly introduced cementitious materials as well as carbon dioxide penetration and reaction rate of carbonation.

Sustainable development driven by society has led to the production of new construction materials with low environmental impact. Nowadays, most countries regularly threaten the emission of carbon dioxide gas to their environments. The worldwide cement industries emit approximately 5% to 7% CO_2, of global CO_2 emissions to the environment [10-11]. These emissions are further increasing due to the rising demand for concrete. In this situation, geopolymer concrete prepared from industrial by-products is an alternative building material to reduce the environmental pollution from cement production. But a limited amount of geopolymer concrete has been implemented into commercial applications, even though many studies have shown that geopolymer is a suitable alternative material to Portland cement [12]. The carbonation problem is the key limiting factor to adopting geopolymer technology in the construction industry [13] since it is prepared from supplementary cementitious materials. Many researchers have found that as the percentage of supplementary cementitious materials increased in concrete the carbonation front also increased simultaneously [14-15]. A service life model has been prepared for concrete prepared by partial replacement of cement with different supplementary cementitious materials and it was found that the carbonation depth was doubled when metakaolin was used compared to that of

concrete without metakaolin after 50 years [16]. As the geopolymer concrete is generally prepared from supplementary cementitious materials, it is necessary to evaluate consequent reinforcement corrosion by comparing the carbonation depth of various geopolymer concretes prepared from supplementary cementitious materials. Hence a suitable concrete ingredient must be found for reducing the carbonation process of geopolymer concrete.

2. Research Significance

In this research, rubber latex is used to improve the corrosion resistance of rebar in geopolymer reinforced concrete. The corrosion of rebar occurs due to both carbonation and chloride attack. Rath et al (2020) found that using rubber latex not only increases the workability of concrete but also improves the microstructure of concrete which can resist liquid permeability [17]. They conducted a bulk electrical resistivity test on calcined clay geopolymer concrete and concluded that natural rubber latex improved the ITZ layer of concrete, which decreased the liquid permeability (i.e. chloride and moisture). But that research was silent about the influence of natural rubber latex on the carbonation of concrete. A limited number of research papers have analyzed the resistance against carbonation of concrete, in which rubber latex has been used for improving concrete performance. The amount of uptake carbon dioxide by the geopolymer concrete and its carbonation depth should be determined with different doses of rubber latex. In this research, a detailed study has been done about the effect of natural rubber latex on calcined clay-based geopolymer concrete against the carbonation reaction. The rubber latex acts as a coating agent and improves the interfacial transition zone (ITZ) of concrete. The resistance capacity of natural rubber latex against carbonation has been verified from ultrasonic pulse velocity (UPV), bulk electrical resistivity (ER), thermogravimetric analysis (TGA), scanning electronic microscope (SEM) image, etc. Ultrasonic velocity and electrical resistivity before carbonation may show the improvement of the ITZ layer by natural rubber latex as compared to traditional concrete, and after carbonation it will indicate that what percentage of voids has been filled by $CaCO_3$. TGA will give the amount of $CaCO_3$ by the loss of mass in the temperature range between 500^0C to 1000^0C [18]. SEM images also indicate the improvement of the ITZ layer before and after carbonation, i.e., indirectly giving a rough idea about the amount of $CaCO_3$ produced which has filled the pores. Rath et al. (2000) explained that the strength of calcined clay based geopolymer concrete had shown lower strength as compared to traditional concrete of the same grade. Also, it has been proved that the fiber cement composite has improved ITZ layer between cement paste and fiber [19]. So, 0.1% of glass fibers have been used to improve its ITZ layer. A mathematical correlation has been developed between the diffusion coefficient of carbon dioxide with ultrasonic pulse velocity and bulk electrical resistivity test results.

3. Materials and Methods

3.1 Preparation of sample and durability test

In this research, calcined clay, sodium hydroxide, calcium silicate, sand, brick aggregate, rubber latex, glass fiber, and water are taken as ingredients for the preparation of geopolymer concrete. The mixed design of traditional concrete and geopolymer concrete has been followed as per the author's previous research [17]. Brick aggregate was used as coarse aggregate and fixed as a maximum size of 20 mm. The ratio of fine aggregate to coarse aggregate is taken as 50:50 by volume. for getting a better packing density [20-21]. A mixture of sodium hydroxide (NaOH) solution and calcium silicate ($CaSiO_3$) solution was used with the ratio of 1:2.5 and alkali activator solution to calcined clay ratio = 0.35. The physical and

chemical properties of the above materials are shown in Table 1, Table 2 and Table 3. Fifteen mixes of M40 grade were prepared for different doses of rubber latex (i.e., 0.5%, 1%, 1.5%, and 2.0% of calcined clay) as an organic admixture, shown in Table 4. To improve the compressive strength capacity of geopolymer concrete, 0.1% of fiber has been added. To compare the carbonation properties of geopolymer concrete with and without reinforced glass fiber, traditional cement concrete of the same grade was also prepared.

Table 1. Physical and Chemical Properties of Different Materials used in Present Research [Rath et al. (2020)].

Sr. No	Material	Properties
1	Cement	Ordinary Portland Cement of 43 grade, fineness = 3%, initial setting time = 70 minutes, final setting time = 500 minutes, compressive strength at 28 days = 45 MPa
2	Calcined clay	Particle sizes are less than 45 microns, specific gravity=2.85, Blain air permeability=410 m^2/kg
3	Brick Aggregate	Prepared by pounding the brickbat, all aggregates are passed through a 20 mm sieve, specific gravity=1.84
4	Sand	Confirmed as Zone-III, specific gravity =2.65
5	NaOH	Procured in terms of tablets from the local market.
6	$CaSiO_3$	Procured in terms of gel and used as an activator such that the ratio between NaOH solution to $CaSiO_3$ gel solution as 1: 2.5
7	Rubber Latex	White liquid procured from the rubber tree
8	Glass fiber	Length of Glass fiber = 12 mm, diameter = 14µm, volume of fraction = 0.1%

Table 2. Chemical Composition of Cementitious Materials [Rath et al. (2020)].

Composition	Calcined Clay	Ordinary Portland Cement
CaO	1.15	68.42
Al_2O_3	17.21	4.95
SiO_2	68.35	17.61
MgO	1.83	1.95
Fe_2O_3	7.37	2.05
Na_2O	1.24	0.25
K_2O	2.57	0.52
SO_3	0.03	2.91
Loss on ignition	0.25	1.34

Table 3. Physical and Chemical Properties of Rubber Latex [Rath et al. (2020)].

Parameters	Values
Appearance	Free-Flowing Liquid
Color	Milky White
Specific Gravity	1.1
pH	8.1
Total solid content	62.84%
Dry rubber content	59.23%
Non-rubber contents	1.4%
Volatile fatty acids	0.016%

After the dry mixing of calcined clay, brick aggregate and sand, prepared sodium hydroxide solution and calcium silicate gel were poured to mix as per mix design. A series of cube specimens with a size of 100 mm X 100 mm X 100 mm were cast to determine the carbonation resistance of concrete cubes. The carbonation resistance of concrete cubes can be evaluated by the carbonation depth of the cube specimen under

the action of CO_2 pressure. Before testing, about 90 cubes (i.e. two sets of 15 mixes) were cast with M40 grade of geopolymer concrete for different doses of rubber latex (i.e. 0.5%, 1%, 1.5% and 2.0% of calcined clay) as shown in Table 4. Three samples were cast in each mix and the averages of test results of those three samples were taken after each test. The first set of 15 mixes was cast for determining the compressive strength, ultrasonic pulse velocity test (UPV) and bulk electrical resistivity test (ER) before carbonation, and the second set of 15 mixes was cast for determining the carbonation depth, compressive strength, ultrasonic pulse velocity test (UPV) and bulk electrical resistivity (ER) after keeping them in a carbonation chamber for 28 days. After 24 hours of casting, the traditional concrete sample (MT) was demoulded and cured in water for 28 days and the surface allowed to dry at normal temperature. Whereas the geopolymer concretes (MG and MGF) were remolded and kept in the oven for three days at 105^0C. Then they were removed from the oven and cured in an open-air atmosphere for 28 days. After that, UPV, ER and compressive strength tests were conducted on one set cubes of 15 mixes and other sets of cubes of 15 mixes were kept in the carbonation chamber for 28 days.

Table 4. Mix Proportions of Concrete.

Mix	Cement (kg/m^3)	Calcined Clay (kg/m^3)	Sand (kg/m^3)	Stone Aggregate (kg/m^3)	Brick Aggregate (kg/m^3)	NaOH (kg/m^3)	$CaSiO_3$ (kg/m^3)	Fiber (kg/m^3)	Extra Water (kg/m^3)	Rubber Latex (kg/m^3)	Slump Height (mm)	pH value (before carbonation)
MT_0	415	0	920	960	0	0	0	0	170	0	35	14.0
MG_0	0	415	625	0	1150	45	113	0	115	0	28	12.4
MGF_0	0	415	625	0	1150	45	113	2.7	115	0	15	12.4
$MT_{0.5}$	415	0	920	960	0	0	0	0	170	2.08	43	13.5
$MG_{0.5}$	0	415	625	0	1150	45	113	0	115	2.08	33	12.7
$MGF_{0.5}$	0	415	625	0	1150	45	113	2.7	115	2.08	17	12.7
$MT_{1.0}$	415	0	920	960	0	0	0	0	170	4.15	52	13.6
$MG_{1.0}$	0	415	625	0	1150	45	113	0	115	4.15	39	13.1
$MGF_{1.0}$	0	415	625	0	1150	45	113	2.7	115	4.15	20	13.1
$MT_{1.5}$	415	0	920	960	0	0	0	0	170	6.23	60	13.7
$MG_{1.5}$	0	415	625	0	1150	45	113	0	115	6.23	47	13.3
$MGF_{1.5}$	0	415	625	0	1150	45	113	2.7	115	6.23	23	13.3
$MT_{2.0}$	415	0	920	960	0	0	0	0	170	8.32	69	13.7
$MG_{2.0}$	0	415	625	0	1150	45	113	0	115	8.32	53	13.5
$MGF_{2.0}$	0	415	625	0	1150	45	113	2.7	115	8.32	27	13.5

where,
MT: Traditional Cement Concrete Mix
MG: Geopolymer Concrete Mix (Calcined clay-based with Brick Aggregate)
MGF: Fibre Reinforced Geopolymer Concrete (Calcined clay-based with Brick Aggregate)
The suffix number attached with each code of mix denoted as percentage rubber latex added to that corresponding mix.

The concentration of carbon dioxide was kept at 5%, temperature 35^0C and 70% humidity. After the curing period, they were taken out from the carbonation chamber and UPV, ER and compressive strength tests were again determined for each mix. After taking the compressive strength of all specimens, all the half-broken (cracked) cubes were made into two halves and a 1% phenolphthalein solution was applied to the broken surface. After some time, pink color was seen in an uncarbonated portion of concrete and no color change was observed in carbonated concrete. The carbonation depth

(CD) was measured by using a measuring scale and tabulated in Table 5 with the compressive strength before carbonation and after carbonation.

Table 5. Carbonation depth and compressive strength of different mixes before and after carbonation.

Mix	Carbonation Depth (mm)	Before Carbonation			After Carbonation		
		UPV (km/s)	ER (kΩ cm)	Comp St. (MPa)	UPV (km/s)	ER (kΩ cm)	Comp St. (MPa)
MT_0	2.5	5.16	8.61	40.51	5.24	9.90	47.74
MG_0	3.8	5.19	8.92	38.29	5.26	10.08	43.27
MGF_0	2.1	5.28	10.23	43.25	5.37	11.97	50.60
$MT_{0.5}$	2.2	5.21	9.17	42.14	5.29	10.64	48.88
$MG_{0.5}$	3.6	5.22	9.43	40.21	5.29	10.75	46.98
$MGF_{0.5}$	1.9	5.39	12.91	45.73	5.49	15.23	53.96
$MT_{1.0}$	1.8	5.32	11.29	44.92	5.41	13.10	52.11
$MG_{1.0}$	3.3	5.38	11.95	42.75	5.46	13.62	48.74
$MGF_{1.0}$	1.6	5.53	16.98	49.28	5.63	20.04	58.15
$MT_{1.5}$	1.5	5.44	13.75	48.05	5.53	16.09	52.85
$MG_{1.5}$	3.1	5.46	14.81	45.96	5.54	17.03	52.85
$MGF_{1.5}$	1.3	5.93	22.11	52.91	6.04	26.31	62.96
$MT_{2.0}$	1.3	5.52	16.74	49.23	5.62	19.75	58.09
$MG_{2.0}$	2.8	5.75	18.32	47.38	5.84	21.25	54.96
$MGF_{2.0}$	1.0	6.14	25.96	57.27	6.20	28.56	63.00

3.2 Amount of carbon dioxide uptake by different mixes

The mass of the percentage of carbon dioxide uptake by concrete samples was determined considering the difference in weight of concrete cubes before carbonation and after carbonation. The mass gain was determined by

$$Mass\ gain(\%) = \frac{Mass_{final} - Mass_{initial}}{Mass_{cementitious\ materials}}.$$

The water and activators were included in this calculation because the whole process was conducted in a closed process and water participates in chemical reaction forming calcium carbonate (for traditional cement concrete) and aluminum hydroxide (for geopolymer concrete). But the aggregates are excluded since they do not absorb carbon dioxide. This is validated by using mass gain due to the uptake of carbon dioxide at the process of carbonation by using Berger's pyrolysis approach [22]. About 50 gm of carbonated samples were kept in a ceramic crucible and placed inside the oven at 105^0C. By this process, the uncombined water was removed. Again, the samples were heated in a muffle furnace to 550^0C to 1000^0C. It can be understood that the mass loss from 105^0C to 550^0C associated with the loss of chemical bound water which has been participated in the hydration process. The further loss of mass at temperature raised from 550^0C to 1000^0C is associated with chemically bound carbon dioxide (i.e. calcium carbonate). The amount of carbonate content (i.e. loss mass due to ignition process) is approximately equal to the amount of carbon dioxide uptake by concrete surface [23]. It was found that the amount of carbon dioxide uptake by traditional as well as geopolymer concrete mixes was the same by the above two processes with a 10% difference. The percentage of carbon dioxide absorbed in different mixes is shown in Fig. 1. Again, the amount of carbon dioxide is also validated by the analytical method with a variance of 10%.

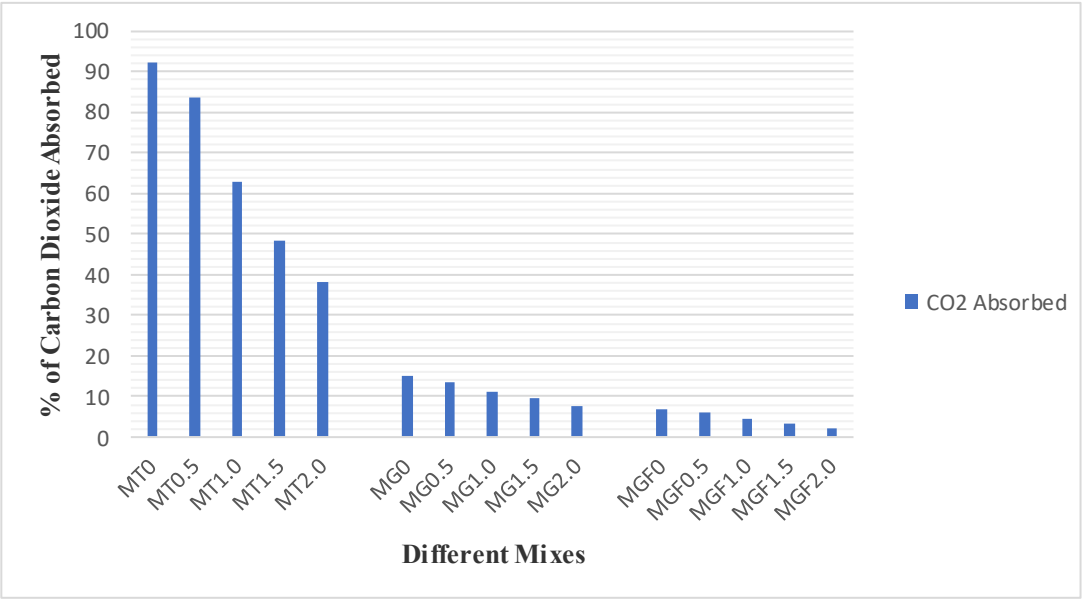

Fig. 1. Percentage of Absorption of CO_2 by Different Mixes.

3.3 Major constituents solubility

By using the U.S. EPA method, the contacting aqueous phase as a function of pH was determined for different mixes of geopolymer concrete [24]. Also, carbonate alkalinities have been estimated by using an acid-base titration curve. The above test was conducted for each carbonated and non-carbonated concrete sample of each mix. Calcium, aluminium and silicon concentrations for each concrete sample were determined with the help of inductively couple plasma-optical emission spectrometry (ICP-OES) as per U.S. EPA Method 6010C. For each material, the titration curve was derived based on the amount of acid added (mol_{H+}/kg-dry). The contribution of hydroxide alkalinity was estimated from the inflection point near pH 8.3 to a pH 4.5 as the acid addition. The contribution of carbonate was considered as the addition of acid from an inflection point near a pH of 8.3 to a pH of 4.5 of each mix. The inorganic carbon present in the carbonate was calculated from each material according to the carbonate alkalinity. Total hydroxide and carbonated alkalinities were calculated from the titration curve for each type of mix. Fig. 2 and Fig. 3 show the titration curves with the hydroxide and carbonate alkalinities regions of different mixes before and after carbonation. The estimation of uncertainties related to the determination of hydroxide, carbonate, and total alkalinity, the inorganic carbon, and solubilities were found according to the mean coefficient of variation across all mixes shown in Table 7.

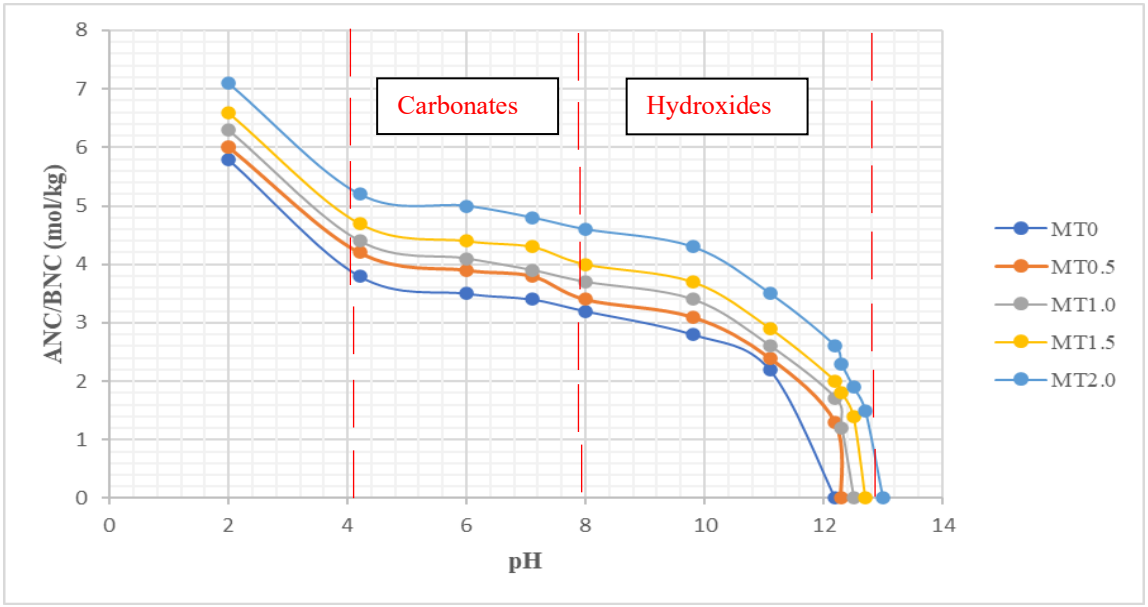

Fig. 2. Titration Curve Generated for Traditional Mixes varies with Different Percentages of Rubber Latex before Carbonation.

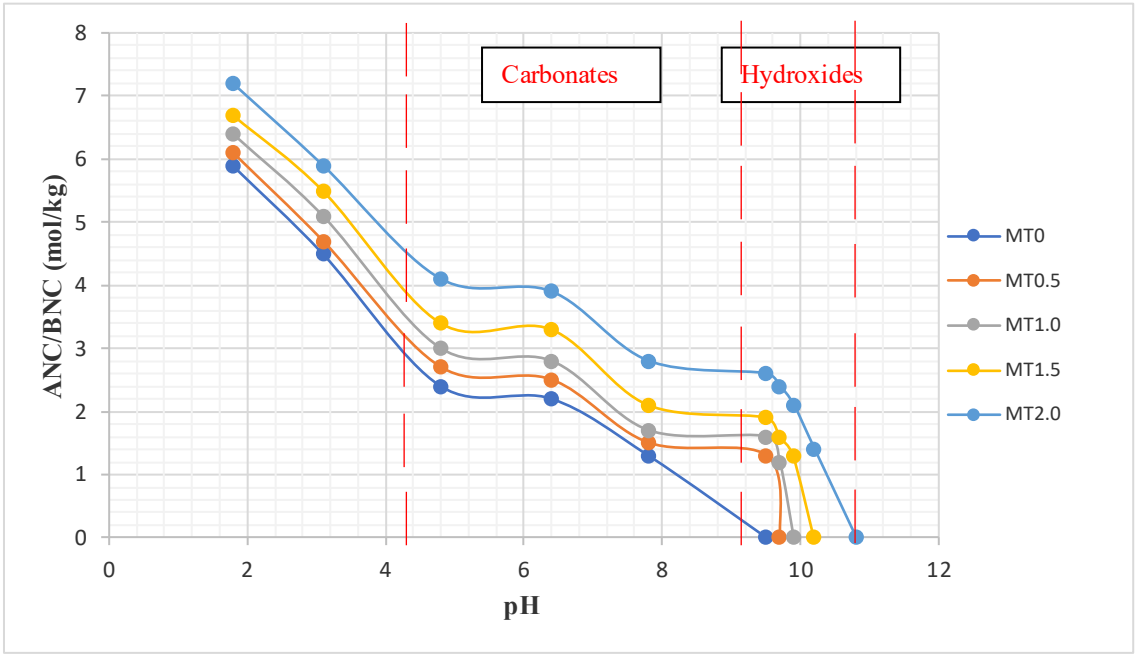

Fig. 3. Titration Curve Generated for Traditional Mixes varies with Different Percentages of Rubber Latex after Carbonation.

Note: ANC/BNC: Acid/Base Neutralisation Capacity

Table 6. Percentage of Mass of C-S-H, C-A-S-H and $CaCO_3$ before Carbonation and after Carbonation according to the Weight Loss of the DTG Curve w.r.t Temperature Ranges.

Mix	Before Carbonation			After Carbonation			
	C-S-H (%)	C-A-S-H (%)	$CaCO_3$ (%)	C-S-H (%)	C-A-S-H (%)	$CaCO_3$ (%)	TGA (solid)
MT-0	15.4	---	2.1	12.3	---	6.8	1.3
MG-0	---	14.2	1.3	---	9.8	9.2	1.7
MGF-0	---	14.2	1.3	---	10.6	7.2	1.5
MT-0.5	15.4	---	2.1	12.7	---	6.4	1.2
MG-0.5	---	14.2	1.3	---	10.0	8.8	1.6
MGF-0.5	---	14.2	1.3	---	10.9	6.7	1.4
MT-1.0	15.4	---	2.1	13.2	---	5.9	0.9
MG-1.0	---	14.2	1.3	---	10.3	8.3	1.4
MGF-1.0	---	14.2	1.3	---	11.4	6.2	1.2
MT-1.5	15.4	---	2.1	13.8	---	5.3	0.6
MG-1.5	---	14.2	1.3	---	10.7	7.8	1.1
MGF-1.5	---	14.2	1.3	---	11.9	5.6	0.9
MT-2.0	15.4	---	2.1	14.4	---	4.7	0.3
MG-2.0	---	14.2	1.3	---	11.1	7.2	0.7
MGF-2.0	---	14.2	1.3	---	12.6	4.8	0.5

Table 7. Service Life Period for Various Mixes.

Mix	K(Ωcm3/year)	ρ (kΩ cm)	r	CD (mm)	X (cm)	t (years)
MT_0	5000	8.61	1.8	2.5	2.75	101.05
MG_0	5000	8.92	1.8	3.8	2.62	95.02
MGF_0	2850	10.23	1.8	2.1	2.79	216.81
$MT_{0.5}$	5000	9.17	1.8	2.2	2.78	109.98
$MG_{0.5}$	5000	9.43	1.8	3.6	2.64	102.00
$MGF_{0.5}$	2850	12.91	1.8	1.9	2.81	277.54
$MT_{1.0}$	5000	11.29	1.8	1.8	2.82	139.33
$MG_{1.0}$	5000	11.95	1.8	3.3	2.67	132.21
$MGF_{1.0}$	2850	16.98	1.8	1.6	2.84	372.88
$MT_{1.5}$	5000	13.75	1.8	1.5	2.85	173.32
$MG_{1.5}$	5000	14.81	1.8	3.1	2.69	166.31
$MGF_{1.5}$	2850	22.11	1.8	1.3	2.87	495.84
$MT_{2.0}$	5000	16.74	1.8	1.3	2.87	213.98
$MG_{2.0}$	5000	18.32	1.8	2.8	2.72	210.34
$MGF_{2.0}$	2850	25.96	1.8	1	2.9	594.41

3.4 Thermogravimetric analysis

After 28 days of curing, each mix of the concrete specimen was ground into a powder and heated about 800 ^{0}C at a constant rate of heating 10 ^{0}C/min. For estimating the mass fraction of C-S-H (for MT mix), C-A-S-H (For MG and MGF mix) and their respective carbonation products of various mixes, a thermogravimetric instrument was used. The amount of calcium carbonate in geopolymer fiber (MGF) and non-fiber reinforced concrete (MG) prepared from calcined clay as well as traditional concrete (MT) prepared from OPC were determined from the loss of mass between temperature 520 ^{0}C to 750 ^{0}C. The temperature range was found on the observations of the peak due to loss of mass for all types of mixes. Apart from it, TGA results were used to determine the reaction capacity of calcium

during the carbonation process, i.e., the ratio of calcium that reacted during the carbonation process at lab practice to the theoretical amount.

3.5 Carbonic service life period

The life period of concrete depends upon the resistance of the corrosion of rebar inside the concrete. The corrosion of reinforcement in concrete may accelerate due to the diffusion of carbon dioxide gas in concrete. Carbon dioxide can penetrate the concrete by a diffusion process without the existence of major cracks. The diffusion coefficient of concrete is a time-dependent function that continues parallel to the hydration process. Carmen Andrade (2010), proposed a relation between electrical resistivity (ρ) and service life period (t) with cover depth (x_c) of a structural member as follows:

$$x_c = \sqrt{\frac{K}{\rho_0 \left(\frac{t_e}{t_0}\right)^q r_{cl}}}\sqrt{t}.$$

In this experiment following parametric values are taken for the above formula. x_c = Un carbonated cover depth = (30 – carbonation depth) in mm. K = Coefficient of carbon dioxide permeability $= 5{,}000 \frac{\Omega cm^3}{year}$ for non – fiber reinforced concrete $= 2{,}850 \frac{\Omega cm^3}{year}$ for fiber reinforced concrete. ρ_0 = Electrical resistivity at 28 days (From Table 5). t_e = 10 years. t_0 = 28 days = 0.0767 years. q = Aging factor during 10 years = 0.3. r_{cl} = Cement binding factor = 1.8. t = Life time or service life period.

The carbonic service life period of fifteen different mixes is determined by using the above formula. Since the concrete surfaces continuously contact with water and environmental condition is cyclic wet and dry, the type of exposer class for the concrete of this research is assumed as x_{c3}. The coefficient of carbon, dioxide permeability is 3000 Ωcm^3/year for cyclic wet and dry [25]. But in the carbonation chamber, the exposer condition is too much higher than the environmental condition. Hence, K value is considered as 5000 Ωcm^3/year. According to Bhargava and Banthia (2007), the coefficient of permeability (K) for a 0.1% volume of a fraction of fiber reinforced concrete is approximately 0.57 times that of plain concrete. Hence the value of K is taken as 2850 Ωcm^3/year for fiber reinforced concrete. Generally, the clear cover of the structural member is taken as 30 mm. Here the term X is taken as uncarbonated cover depth, i.e., 30 mm - carbonation depth of concrete and tabulated in Table 5 for various mixes.

4. Results and Discussion

4.1 Carbon dioxide uptake and pH analysis

Again, from Table 4 it is found that the pH value of traditional concrete is more than the geopolymer concrete because calcined clay had a lower amount of alkalinity (8.3) as compared to OPC (12.7). But the pH value of geopolymer concrete without rubber latex increased up to 12.4 because of alkali activator $CaSiO_3$ and NaOH solution. Among the non-fiber reinforced concrete mix, the high alkalinity content mix ($MT_{2.0}$) resulted in a carbonated material having the smallest depth of carbonation. The highest penetration depth was observed at a low alkalinity content mix (MG_0) which indicates the depth of carbonation is inversely proportional to the amount of alkalinity content in concrete. The hydroxide alkalinity differences in non-carbonated concrete mixes indicate that different reactive capacities exist across the different materials to react with CO_2 [8]. But the addition of fiber plays a mechanical role to seal the pores of the concrete surface structure and reduces the carbonation depth. Again, it is found that

when 2% of rubber latex was used as an admixture, the pH value of geopolymer concrete increased as 6.8%. Also, the carbonation depth decreased as 26%, after adding rubber latex of 2% in geopolymer concrete. It indicates that the use of rubber latex in concrete not only increases the workability, rheological property and strength, but also increases the alkalinity of concrete; which provides strength to the passivation layer surrounding the rebar. It can be noticed that during the carbonation process the hydroxide alkalinity of traditional concrete was continuously reduced whereas the carbonate alkalinity was continuously increased. But the pH value of $CaCO_3$ was 8.35 which was less than the pH value of $Ca(OH)_2$ whose pH was 11.27 [(26)]. Hence, the reduction of alkalinity percentage decreased in traditional concrete due to simultaneously increasing of the percentage of calcium carbonate and decreasing of the percentage of calcium hydroxide. But in calcined clay based geopolymer concrete, the amount of alumina in calcined clay was 3.5 times higher than the OPC (Table 2). Therefore, after the carbonation process a higher amount of aluminium hydroxide was produced by depleting calcium hydroxide. The pH value of aluminium hydroxide was 7.4[(27)]. Due to this reason, the pH value of calcined clay based geopolymer concrete was less than the traditional concrete of all mixes. But when the rubber latex was added in geopolymer concrete up to 2% as an admixture, the initial pH value of geopolymer concrete was increased at a fresh state before carbonation. Also, it filled the pores of the concrete and sealed them at the hardening stage. As a result, the ITZ layer of concrete became improved and diffusion of carbon dioxide on the concrete surface was resisted up to 50% successfully. Thus, it is recommended that a higher percentage of rubber latex should be added to high alumina based geopolymer concrete to reduce the carbonation depth.

4.2 Carbonation depth of different mixes

From Table 5 it can be seen that the carbonation depth is more in geopolymer concrete than traditional cement concrete of the same mix. This happens due to a decreasing pH level in geopolymer concrete compared to traditional cement concrete after the carbonation process. In traditional concrete, the $Ca(OH)_2$ comes into contact with CO_2 and is converted into $CaCO_3$, which decreases the pH level from 14 to 12. But in geopolymer concrete, $Al(OH)_2$ forms after the carbonation process, whose pH value is near 7. Hence, the pH value of geopolymer non-fiber reinforced concrete is less than the traditional concrete. But when fibers were mixed in concrete, most of the pores and shrinkage cracks developed on the surface of concrete were sealed by the fibers. A much lower amount of carbon dioxide gas was absorbed by the concrete surface as shown in Fig. 1 and entered inside the concrete through pores. This results in a smaller depth of carbonation in fiber reinforced concrete than in the traditional concrete for all doses of rubber latex. Also, the hardened properties of rubber latex helped to close the pores on the surface of the concrete by forming a coating on the external surface. When the rubber latex was mixed with concrete it was in the liquid stage, but after some time elapses, the rubber latex becomes hard and tries to seal the pores of concrete at the interfacial transition zone. Thus, alkali-silica reaction or delayed ettringite reaction is unable to form any surface crack and the acceleration of the carbonation process was resisted. It was found that as the percentage of rubber latex was increased the carbonation depth also significantly decreased. Again, it was seen that all the test results of hardened concrete such as UPV, ER and compressive strength are better after carbonation than the test results from before carbonation. It indicates that the calcium carbonate formed during the carbonation process filled all capillary pores.

4.3 TGA analysis

Fig. 4 shows the test result of thermogravimetric for mix MG_0. It can be noticed that the loss of weight of samples of each mix increased as the temperature increased. In the TGA curve, it can be seen that loss of mass is very slow at temperature ranges from 150 ºC to 400 ºC in the first region. The decomposition of C-A-S-H is shown by a peak near 400 ºC for mix MG_0 before carbonation and after carbonation. A sharp peak near temperature ranges of 400 ºC to 500 ºC indicates the decomposition of portlandite evident for MG_0 before carbonation. However, near the above temperature zone, no peak was found for carbonated MG_0. Again, for carbonated mix MG_0, a peak is formed near the range of temperature 650 ºC to 750 ºC. The low-rise peak of carbonate peak may be due to the decomposition of calcite formed from the vaterite heating. But the beginning of the sharp peak may be due to the loss of carbon dioxide from the dissociation of calcite at the carbonation period. The rapid declination of weight occurred when the temperature reached 200 ºC due to loss of free water [28-29]. From 200 ºC to 800 ºC temperature all the mixes experienced gradual loss of weight due to the evaporation of chemically combined water which occurred up to reaching 300 °C temperature[30].

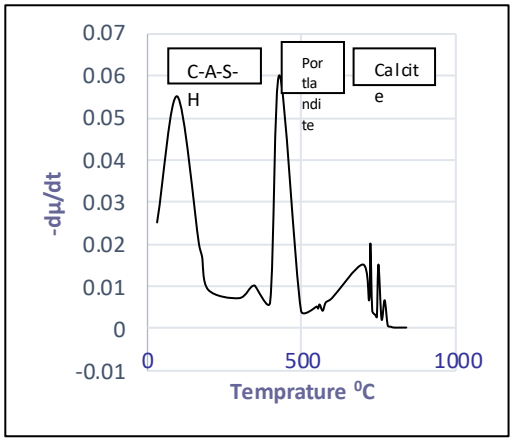

(a) DTG Curve of Uncarbonated Mix MG-0

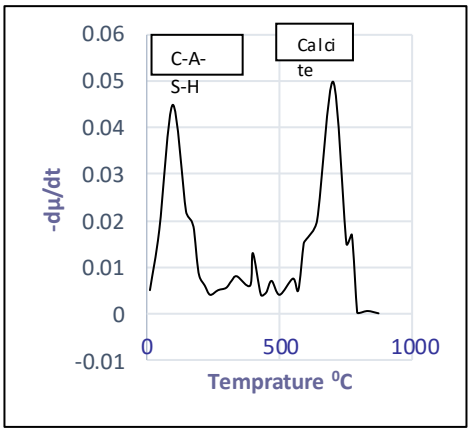

(b) DTG Curve of Carbonated Mix MG-0

Fig. 4. TGA Result between Temperature and Derivative of mass w.r.t Temperature for Uncarbonated and Carbonated Geopolymer Concrete.

From Table 7 it can be noticed that each sample shows the presence of $CaCO_3$ in a small amount before carbonation. This might be due to the contact of atmospheric carbon dioxide at the time of casting and during the curing period. The percentage of the mass of different phases derived from the loss of mass associated with the given temperature changes. The rate of reaction of calcium was inversely proportional to the alkalinity of the concrete ingredients. Again, it can be seen that after carbonation the calcite increased to 3.23 times more than before carbonation for mix MT_0 but it increased 7.07 and 5.53 times than after carbonation of mixes MG_0 and MGF_0, respectively. Due to the addition of fiber in geopolymer concrete, the diffusion of carbon dioxide decreased followed by the carbonation process also decreased significantly. It has been proved that when the fibers are used in concrete, the interfacial transition zone of concrete has been improved due to the strong bond between cement paste and fiber (31). It significantly improved the tensile strength of the fiber-cement composite, resisted potential cracking, and helped to reduce the gas and liquid permeability.

4.4 SEM image analysis

In the SEM image (Fig. 5) one can see that the densification of ITZ is greater after carbonation than before carbonation. Also, the author found that as the percentage of rubber latex was increased up to 2% in calcined clay based geopolymer concrete mix, the liquid rubber latex partially filled up surface voids and porosity coated on the surface of oxides of the cementitious particle as well as aggregate particles (17). After the hardening of liquid rubber latex, a coating is formed around the coarse aggregate. The interfacial transition zone of concrete improved due to the combined effect of hardening of rubber latex and an extra amount of C-A-S-H gel formed due to releasing of water from the saturated brick aggregate. Hence, the microstructure of the SEM image of mix $MG_{2.0}$ is denser than the microstructure of SEM image MG-0 (17). But now it is found that the microstructure of the SEM image of mix $MG_{2.0}$ after carbonation became densest by filling remaining pores with $CaCO_3$ which is shown in Fig. 3. Also, UPV and ER values are higher when concrete contains 2% rubber latex of cementitious materials. The amount of cloud structure is very small in mix MG_0 (Fig. 5(a)), but it is more in the amount shown in mix $MG_{2.0}$ after carbonation (Fig. 5(c).). Also, the carbonation area becomes lighter shade; whereas the uncarbonated area becomes a darker shade. The geopolymer concrete with 2% rubber latex shows the consistent depth of carbonation across the surface area; however, a smaller area of carbonation not connected to the bulk carbonation front is observed at a deeper level in the material and between two large aggregates. A preferential diffusion pathway through the material pore structure during the carbonation process indicates this remote carbonation zone.

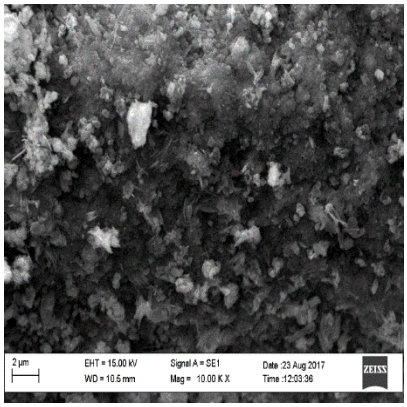

(a) SEM image of Mix MG_0 (before carbonation) [Rath et al.(2020)].

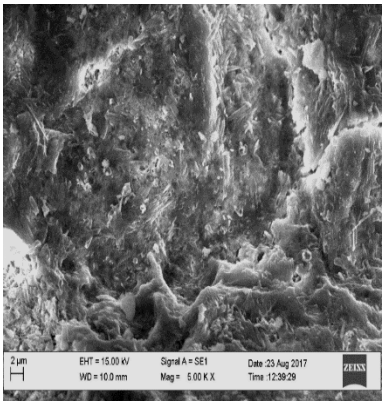

(b) SEM image of Mix $MG_{2.0}$ (before carbonation) [Rath et al. (2020)].

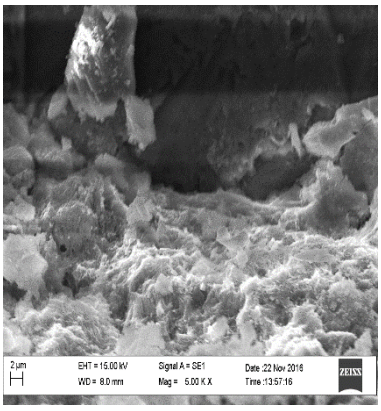

(c) SEM image of Mix $MG_{2.0}$ (after carbonation)

Fig. 5. SEM Image of Geopolymer Concrete with and without Rubber Latex before and after Carbonation.

4.5 Carbonic service life period

From Table 5 it can be noticed that the service life period of the carbonation of geopolymer concrete is 6% less than the service life period of traditional concrete. But when 0.1% fiber is added to geopolymer concrete, the service life period becomes twice that of traditional concrete. This indicates that 0.1% of glass fiber is able to resist the diffusion of carbon dioxide. Thus, it is strongly recommended that up to 0.1% glass fiber be used in geopolymer concrete to increase the service life period of the structure. Also, it can be noticed that as the percentage of rubber latex increased up to 2% the service life period of concrete nearly doubled. The addition of rubber latex improved the ITZ layer and decreased the porosity and rate of diffusion of carbon dioxide gas.

4.6 Playing a role of rubber latex as coating material

In the present research, rubber latex was used as a performance improver of both traditional cement concrete and geopolymer concrete. The rubber latex shows dual character, i.e., it is available in liquid form at the time of collection from the rubber tree and it becomes solid after the passing of time. This property helped to improve the performance of concrete in current research. When the liquid rubber latex was added to concrete it became soluble with water easily and filled the voids of the cement or cementitious particles of concrete. The rubber latex enabled making concrete mixtures of the required consistency and forms a film around them in the fresh stage. That film created an opposite charge and repelled the adjacent cement particles one from each other. Also the inserted polymer particles in between two cementitious particles provided ball-bearing action. Hence the workability, as well as flowability of concrete, increased. The rubber latex polymer helped to accelerate the polymerization process of geopolymer concrete. The rubber latex was ionized in the highly alkaline environment of fresh concrete and tends to interact with calcium ions of cement hydrates. It improved the stability of polymer latex and higher bond strength between the rubber latex modified concrete and the existing substrates. As time elapsed the concrete set and the liquid rubber latex became solid. The film of rubber latex interwove the cement hydrates and formed a monolithic polymer cement matrix structure at the interface, bridging the pores and cracks on it. Thus, a hard coating was formed on the top surface of the concrete which improved the ITZ layer found from the SEM image. As a result, both UPV and ER test results showed higher values for higher percentage rubber latex dosed concrete. The hard surface coating layer of rubber latex resisted the entering of carbon dioxide through the concrete surface. As the percentage of rubber latex added into the concrete increased, the amount of penetration of carbon dioxide decreased due to the improvement of the ITZ layer. Hence, the formation of carbonic acid also decreased showing a lower value of carbonation depth. It was also proved through TGA analysis as the solid residue was greater for a higher percentage of rubber latex was used. In rubber latex based concrete two types of bond were found. The first one is the bond between two cementitious particles and the second one is the bond between cementitious particles and rubber latex polymer. The bond between the cementitious particle and rubber latex was stronger than the bond between the two cementitious particles. When the rubber latex polymer content was increased, the polymer film covered the hydrated cement and aggregates forming several cementitious particles-rubber latex polymer bonds. These results improved the strength as well as the carbonic service life period of the modified sample.

5. Mathematical Correlation between UPV, ER and Diffusion Coefficient of Carbon Dioxide

The supplementary cementitious materials bearing with alumina used in geopolymer concrete C-A-S-H gel is formed instead of C-S-H gel. These changes in composition can also affect carbonation. The alkali-activated concretes not containing calcium hydroxide will progress directly to carbonation of the key strength-giving binder products like C-A-S-H gel and formed the carbonic acid, which filled the pores.

The diffusion of carbon dioxide occurs through the cement matrix at the time of the carbonation of concrete. The CO_2 dissolution into pore solution makes carbonic acid react with calcium hydroxide according to equation (5.1) and the secondary reaction occurs with calcium silicates and calcium aluminates as shown in equation (5.2) and equation (5.3) [3].

$$Ca(OH)_2 + CO_2 \rightarrow CaCO_3 + H_2O, \quad (5.1)$$

$$3CaO2Si_2 3H_2O \rightarrow 3CaCO_3 + 2SiO_2 + 3H_2O, \quad (5.2)$$

$$4CaO2Al_2O_3 13H_2O + 4CO_2 \rightarrow 4CaCO_3 + 2Al(HO)_3 + 10H_2O. \quad (5.3)$$

From equation (5.3) it can be concluded that calcium is taking part in the formation of carbonate compound, not aluminium in geopolymer concrete. But it takes part in the entire carbonation process and forms Al $(OH)_3$, which has a lower pH value than Ca $(OH)_2$ [32]. Hence, the carbonation depth is greater in geopolymer concrete than in cement concrete.

In traditional cement concrete, it has been found that the calcium carbonated cement concrete is generally formed from CaO present in Portland cement clinker [33]. Similarly, the calcium oxide and alumina present in cementitious materials used in geopolymer concrete will play the main role in the carbonation process. The carbonation depth is greater due to the presence of alumina than calcium oxide in cementitious material [34]. Thus, the amount of carbon dioxide absorbed per volume for complete carbonated concrete depends upon the weight fraction of calcium oxide and aluminium oxide present in cementitious materials. The equation of Pade and Guimaraes (2007) can be written as

$$a = K \times C \times CaO \times \frac{M_{CO_2}}{M_{CaO}}, \quad (5.4a)$$

[For Traditional Cement Concrete]

$$a = K \times C \times CaO \times \frac{M_{CO_2}}{M_{CaO}} \times \frac{M_{CO_2}}{M_{Al_2O_3}}, \quad (5.4b)$$

[For Geopolymer Concrete]

where a = Amount of carbon dioxide absorbed per volume at time t in $\frac{g}{cm^3}$,

C = Amount of cementitious materials (i.e. calcined clay) in $\frac{kg}{m^3}$,

CaO = Amount of CaO per weight of cementitious materials,

Al_2O_3 = Amount of Al_2O_3 per weight of cementitious materials,

M_{CO_2} = Molar mass of CO_2,

M_{CaO} = Molar mass of CaO,

K = Percentage of calcium oxide will be consumed by the carbonation process. It was found that 75% of the CaO by weight in the Portland clinker is consumed by the carbonation process [33]. Also, it is validated from our experiment which is shown in Table 8. But the percentage of Al_2O_3 by weight that takes part in the carbonation process is unknown. The amount of carbon dioxide uptake by the concrete during carbonation is defined by Yang et al. (2014) as follows:

$$I_{CO_2}(t) = aA_{sf}x_c, \quad (5.5)$$

$$I_{CO_2}(t) = \mathrm{K} \times \mathrm{C} \times \mathrm{CaO} \times \frac{M_{CO_2}}{M_{CaO}} A_{sf} x_c, \qquad (5.5a)$$

[For Traditional Cement Concrete]

$$I_{CO_2}(t) = \mathrm{K} \times \mathrm{C} \times \mathrm{CaO} \times \frac{M_{CO_2}}{M_{CaO}} \times \frac{M_{CO_2}}{M_{Al_2O_3}} A_{sf} x_c, \qquad (5.5b)$$

[For Geopolymer Concrete]

where $I_{CO_2}(t)$ = Amount of carbonation inhaled by concrete in gm,

a = Amount of carbon dioxide absorbed per volume at time t in $\frac{g}{cm^3}$,

A_{sf} = Surface area of concrete cube in cm^2,

x_c = Carbonation depth of concrete at time t.

The value of K can be determined by equating the amount of carbon dioxide uptake by concrete during the carbonation process obtained from equations (5.5a) and (5.5b) with the amount of carbon dioxide absorbed by concrete in the carbonation chamber from the experiment (Table 8).

Table 8. Value of K for Different Mixes.

Mix	C $\left(\frac{gm}{cm^3}\right)$	CC $\left(\frac{gm}{cm^3}\right)$	CaO (%by weight)	Al_2O_3 (%by weight)	M_{CO_2} $\left(\frac{gm}{mol}\right)$	M_{CaO} $\left(\frac{gm}{mol}\right)$	$M_{Al_2O_3}$ $\left(\frac{gm}{mol}\right)$	$\frac{M_{CO_2}}{M_{CaO}}$	$\frac{M_{CO_2}}{M_{Al_2O_3}}$	A_{sf} (cm^2)	Xc (cm)	I (gm)	Amount of CO_2 absorbed (gm)	K
MT_0	0.413	0	68.42	4.95	44	56.077	101.96	0.784	0.431	100	0.25	554.291	415.7	0.75
MG_0	0	0.413	1.15	17.21	44	56.077	101.96	0.784	0.431	100	0.38	105.172	63.1	0.6
MGF_0	0	0.413	1.15	17.21	44	56.077	101.96	0.784	0.431	100	0.21	58.121	29.1	0.5
$MT_{0.5}$	0.413	0	68.42	4.95	44	56.077	101.96	0.784	0.431	100	0.22	487.776	346.3	0.71
$MG_{0.5}$	0	0.413	1.15	17.21	44	56.077	101.96	0.784	0.431	100	0.36	99.637	55.8	0.56
$MGF_{0.5}$	0	0.413	1.15	17.21	44	56.077	101.96	0.784	0.431	100	0.19	52.586	24.7	0.47
$MT_{1.0}$	0.413	0	68.42	4.95	44	56.077	101.96	0.784	0.431	100	0.18	399.090	259.4	0.65
$MG_{1.0}$	0	0.413	1.15	17.21	44	56.077	101.96	0.784	0.431	100	0.33	91.334	45.7	0.5
$MGF_{1.0}$	0	0.413	1.15	17.21	44	56.077	101.96	0.784	0.431	100	0.16	44.283	19.0	0.43
$MT_{1.5}$	0.413	0	68.42	4.95	44	56.077	101.96	0.784	0.431	100	0.15	332.575	199.5	0.6
$MG_{1.5}$	0	0.413	1.15	17.21	44	56.077	101.96	0.784	0.431	100	0.31	85.798	39.5	0.46
$MGF_{1.5}$	0	0.413	1.15	17.21	44	56.077	101.96	0.784	0.431	100	0.13	35.980	14.0	0.39
$MT_{2.0}$	0.413	0	68.42	4.95	44	56.077	101.96	0.784	0.431	100	0.13	288.231	158.5	0.55
$MG_{2.0}$	0	0.413	1.15	17.21	44	56.077	101.96	0.784	0.431	100	0.28	77.495	31.8	0.41
$MGF_{2.0}$	0	0.413	1.15	17.21	44	56.077	101.96	0.784	0.431	100	0.1	27.677	9.1	0.33

Note: *C*: Cement, *CC*: Calcined Clay, *CaO*: Calcium Oxide, Al_2O_3: Aluminium Oxide, CO_2: Carbon Dioxide, M_{CO_2} : Molar mass of CO_2 , M_{CaO}: Molar mass of *CaO*, $M_{Al_2O_3}$: Molar mass of Aluminium Oxide, A_{sf}: Surface area, X_c= Carbonation depth, *I*: CO_2 uptake by concrete, *K*: Diffusion coefficient

Again, the carbonation diffusion coefficient depends upon relative humidity, ambient temperature, aggregate cement ratio, total porosity due to water-cement ratio, types of cementitious material, reduction of concrete porosity due to carbonation and the carbon dioxide diffusion coefficient in fresh concrete.

Therefore, the diffusion coefficient can be determined by using the above parameters as

D = Diffusion due to relative humidity * Diffusion due to ambient temperature * Diffusion due to aggregate cement ratio * Diffusion due to water cement ratio * Diffusion due to the reduction of concrete porosity due to carbonation (5.6)

Table 9. Various Equations for Various Diffusion Parameters.

Parameters	Equations	Author	Remarks
Relative Humidity (RH)	$D_{RH} = 23.32\left(1-\frac{RH}{100}\right)^2 \times \left(\frac{RH}{100}\right)^{26}$	Salvoldi et.al. (2015)(Salvoldi, Beushausen, and Alexander 2015)	RH= Relative Humidity
Ambient Temperature (T)	$D_T = D_{Ref} X_e \left[\frac{Q}{\pi}\left(\frac{1}{T_{Ref}}-\frac{1}{T}\right)\right]$	Talukdar et al. (2012)(Talukdar, Banthia, and Grace 2012)	Q =3900 J/mol K, R=8.314J/mol K, T_{Ref}=298K
Aggregate Cementitious material ratio (A/C)	$D_{\frac{A}{f}} = \left(\frac{A}{C}\right)^{0.2}$	Yang et al. (2014)(Yang, Seo, and Tae 2014)	A= Total Aggregate (kg/m^3), C=cementitious material (kg/m^3)
Water cement ratio (w/c)	$D_{\frac{W}{c}} = 2437.7e^{\left(-5.592\frac{W}{c}\right)}$	Van-Loc Ta et al. (2016)(Ta et al. 2016)	Optimum w/c increases the packing density
Reduction of concrete porosity	$D_{CO_2} = 10^{-7} \times 10^{0.025 f_{ck}}$	Papadakis et al. (1991)(Papadakis, Vayenas, and Fardis 1991)	Gas permeability

From Table 9, we can write the diffusion coefficient of carbon dioxide on the surface of the concrete as

$$D = D_{RH} \times D_T \times D_{A/C} \times D_{W/C} \times D_{CO_2}. \quad (5.7)$$

From Equation (5.5) and Equation (5.6) it can be written as

$$I_{CO_2} = D$$

$$K \times C \times CaO \times \frac{M_{CO_2}}{M_{CaO}} A_{sf} x_c = D_{RH} \times D_T \times D_{A/C} \times D_{W/C} \times D_{CO_2} \quad (5.8)$$

(For Traditional Concrete),

$$K \times C \times CaO \times Al_2O_3 \times \frac{M_{CO_2}}{M_{CaO}} \times \frac{M_{CO_2}}{M_{Al_2O_3}} A_{sf} x_c = D_{RH} \times D_T \times D_{A/C} \times D_{W/C} \times D_{CO_2} \quad (5.9)$$

(For Geopolymer Concrete).

Using the above equation, the value of K is calculated for all fifteen mixes and tabulated as shown in Table 8. Again, it can be noticed that, from the above factors except relative humidity and ambient temperature, all factors are indirectly responsible for the packing density of concrete, which affects the diffusivity of carbon dioxide. Both *UPV* and *ER* test results are also proportional to the packing density of concrete. The corresponding equations for calculation for the various coefficient of diffusions are shown in Table 9.

Hence,

$$D_{A/C} \times D_{W/C} \times D_{CO_2} = a(UPV) + b(ER) + c. \quad (5.10)$$

Therefore, the above equation can be written as

$$aX + bY + c = Z, \quad (5.11)$$

where X represents for *UPV* test results, Y represents for *ER* test results, Z represents $\left(\frac{A}{C}\right)^{0.1} 2437.7e^{\left(-5.592\frac{W}{C}\right)} 10^{-7} \times 10^{-0.025 f_{ck}}$. a, b and c are constant factors. By regression analysis values of a, b and c can be found out. The compatibility equations are

$$\sum Z = nc + a\sum X + b\sum Y, \quad (5.12)$$

$$15c + 81.92a + 211.18b = 5.66 \times 10^{-5}, \quad (5.13)$$

$$\sum XZ = c\sum X + a\sum X^2 + b\sum XY, \quad (5.14)$$

$$81.92c + 448.515a + 1173.489b = 0.0003, \quad (5.15)$$

$$\sum YZ = c\sum Y + a\sum XY + b\sum Y^2, \qquad (5.16)$$

$$211.18c + 1173.489a + 3343.643b = 0.0007, \qquad (5.17)$$

The above parameters are taken from Statistical Table 10. By solving the above equation, we have $c = 7.24\times10^{-4}, a = -1.527\times10^{-4}, b = 8.054\times10^{-6}$. Hence the final equation can be written as

$$D = [-1.527\times10^{-4}(UPV) + 8.054\times10^{-6}(ER) + 7.24\times10^{-4}]D_{RH}D_T. \qquad (5.18)$$

6. Validation of the Mathematical Corelation

Fig. 7 represents the comparison of experimental results and those calculated by the present model using a hypothetical line of perfect equality. The point overlapped to the equality line indicates that both calculated and experimental data are superimposed perfectly. Most of the experimental data are lying on the line of equality, which indicates that the predicted coefficient of diffusion is generally higher than the experimental ones. However, most of the results are within ±20% the margin of error. The determination coefficient is determined between fifteen points and the line of equality is determined as $R^2 = 0.87$.

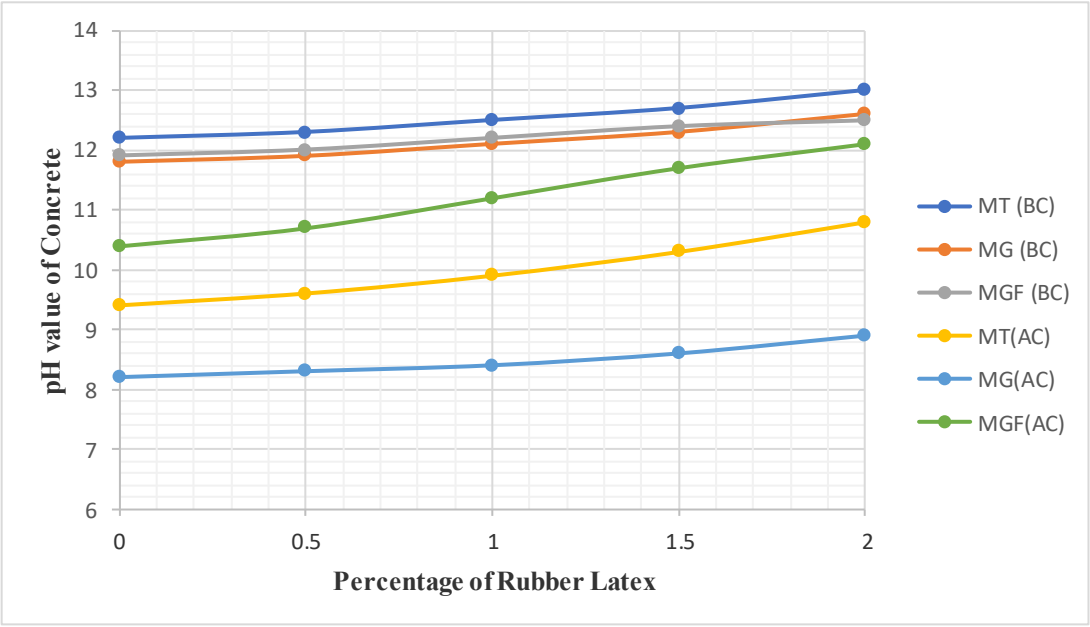

Fig. 6. pH value of Different Mixes before and after Carbonation.

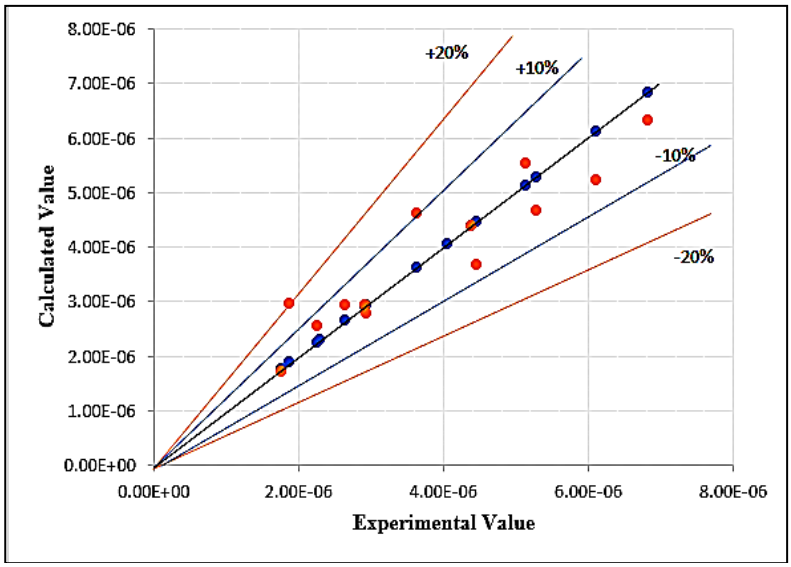

Fig. 7. Comparison between calculated and Experimental Coefficient of Diffusion Value.

Table 10. Statistical Regression Analysis.

Mix	$D_{A/C}$	$D_{W/C}$	D_{CO_2}	Z	X	Y	X^2	Y^2	XY	XZ	YZ
MT_0	1.163	257.541	$9.710X10^{-9}$	$2.91X10^{-6}$	5.16	8.61	26.626	74.132	44.428	$1.501X10^{-5}$	$2.504x10^{-5}$
MG_0	1.156	535.037	$1.103X10^{-8}$	$6.83X10^{-6}$	5.19	8.92	26.936	79.566	46.295	$3.543X10^{-5}$	$6.09X10^{-5}$
MGF_0	1.156	535.037	$8.293X10^{-9}$	$5.13X10^{-6}$	5.28	10.23	27.878	104.653	54.014	$2.709X10^{-5}$	$5.249X10^{-5}$
$MT_{0.5}$	1.163	257.541	$8.840X10^{-9}$	$2.65X10^{-6}$	5.21	9.17	27.144	84.089	47.776	$1.38X10^{-5}$	$2.428X10^{-5}$
$MG_{0.5}$	1.156	535.037	$9.879X10^{-9}$	$6.11X10^{-6}$	5.22	9.43	27.248	88.925	49.225	$3.191X10^{-5}$	$5.764X10^{-5}$
$MGF_{0.5}$	1.156	535.037	$7.190X10^{-9}$	$4.45X10^{-6}$	5.39	12.91	29.052	166.668	69.585	$2.398X10^{-5}$	$5.743X10^{-5}$
$MT_{1.0}$	1.163	257.541	$7.533X10^{-9}$	$2.26X10^{-6}$	5.32	11.29	28.302	127.464	60.063	$1.2X10^{-5}$	$2.548X10^{-5}$
$MG_{1.0}$	1.156	535.037	$8.535X10^{-9}$	$5.28X10^{-6}$	5.38	11.95	28.944	142.803	64.291	$2.841X10^{-5}$	$6.311X10^{-5}$
$MGF_{1.0}$	1.156	535.037	$5.861X10^{-9}$	$3.63X10^{-6}$	5.53	16.98	30.581	288.320	93.899	$2.005X10^{-5}$	$6.158X10^{-5}$
$MT_{1.5}$	1.163	257.541	$6.291X10^{-9}$	$1.88X10^{-6}$	5.44	13.75	29.594	189.063	74.800	$1.025X10^{-5}$	$2.591X10^{-5}$
$MG_{1.5}$	1.156	535.037	$7.095X10^{-9}$	$4.39X10^{-6}$	5.46	14.81	29.812	219.336	80.863	$2.397X10^{-5}$	$6.502X10^{-5}$
$MGF_{1.5}$	1.156	535.037	4.75610^{-9}	$2.94X10^{-6}$	5.93	22.11	35.165	488.852	131.112	$1.745X10^{-5}$	$6.506X10^{-5}$
$MT_{2.0}$	1.163	257.541	$5.878X10^{-9}$	$1.76X10^{-6}$	5.52	16.74	30.470	280.228	92.405	$9.719X10^{-6}$	$2.947X10^{-5}$
$MG_{2.0}$	1.156	535.037	$6.538X10^{-9}$	$4.05X10^{-6}$	5.75	18.32	33.063	335.622	105.340	$2.326X10^{-5}$	$7.412X10^{-5}$
$MGF_{2.0}$	1.156	535.037	$3.700X10^{-9}$	$2.29X10^{-6}$	6.14	25.96	37.700	673.922	159.394	1.406E-05	$5.944X10^{-5}$
			Total	**$5.66X10^{-5}$**	**81.92**	**211.18**	**448.515**	**3343.643**	**1173.489**	**0.000306**	**0.000747**

$Z = D_{A/C} \times D_{W/C} \times D_{CO_2}$.

7. Conclusions

In the present research, the influence of rubber latex on carbonation resistance in both traditional cement concrete and geopolymer concrete has been evaluated. Two aspects were studied. The first one was the diffusivity of carbon dioxide within the bulk paste of rubber latex and calcined clay geopolymer concrete, and the second one was the carbonic life cycle period of concrete with and without rubber latex. It was found that by using rubber latex in geopolymer concrete not only workability of concrete has been increased but also resistance against carbonation increased significantly for both cement concrete and geopolymer concrete. Using rubber latex up to 2% of cementitious material in both cement and geopolymer concrete, the carbonation depth decreases 48% whereas UPV and ER increase up to 8%. The carbon dioxide percentage absorption was found to be seven times greater for traditional cement concrete than geopolymer concrete. This indicates that the microstructure of geopolymer concrete had been developed in a better way as

compared to traditional concrete. The brick aggregate of geopolymer concrete helped in improving the ITZ layer for the formation of more C-A-S-H gel. When the 2% of rubber latex was used in both cement and geopolymer concrete mix, the packing density of concrete increased due to the solidification of rubber latex in between the pores of aggregates at the time of hardening. Hence, the diffusion coefficient of geopolymer concrete decreased. Both UPV and ER values have also a good correlation with the amount of carbon dioxide absorbed by the concrete. The higher values of UPV and ER show a lower amount of carbon dioxide absorption. It has been found that the life cycle period due to carbonation of geopolymer concrete is 6% less than traditional concrete. But when 0.1% glass fiber has been added to concrete, the life cycle period is double that of traditional concrete. Hence it is recommended that 0.1% glass fiber should be added to geopolymer concrete for achieving better durability long service life cycle period. From the above results, it is concluded that rubber latex can be used as a concrete admixture for improving the durability of the concrete structure. Since the admixtures available in the market for improving the performance of concrete are chemical and highly expensive a nonchemical, natural. the non-hazardous, renewable admixture may replace those chemical-based admixtures.

References

[1] Chemrouk M. The deteriorations of reinforced concrete and the option of high performances reinforced concrete. Procedia Eng. 2015;125:713-24.

[2] Andrade C. Propagation of reinforcement corrosion: principles, testing and modelling. Mater Struct. 2019;52(1):2.

[3] Possan E, Thomaz WA, Aleandri GA, Felix EF, dos Santos ACP. CO2 uptake potential due to concrete carbonation: A case study. Case Stud Constr Mater. 2017;6:147-61.

[4] You K, Jeong H, Hyung W. Effects of accelerated carbonation on physical properties of mortar. J Asian Archit Build Eng. 2014;13(1):217-21.

[5] Groves GW, Brough A, Richardson IG, Dobson CM. Progressive changes in the structure of hardened C3S cement pastes due to carbonation. J Am Ceram Soc. 1991;74(11):2891-6.

[6] Badar MS, Kupwade-Patil K, Bernal SA, Provis JL, Allouche EN. Corrosion of steel bars induced by accelerated carbonation in low and high calcium fly ash geopolymer concretes. Constr Build Mater. 2014;61:79-89.

[7] Elsener B, Angst U. Corrosion inhibitors for reinforced concrete. In: Science and Technology of Concrete Admixtures. Elsevier; 2016. p. 321-39.

[8] Branch JL, Kosson DS, Garrabrants AC, He PJ. The impact of carbonation on the microstructure and solubility of major constituents in microconcrete materials with varying alkalinities due to fly ash replacement of ordinary Portland cement. Cem Concr Res. 2016;89:297-309.

[9] Chang C-F, Chen J-W. The experimental investigation of concrete carbonation depth. Cem Concr Res. 2006;36(9):1760-7.

[10] Huntzinger DN, Eatmon TD. A life-cycle assessment of Portland cement

manufacturing: comparing the traditional process with alternative technologies. J Clean Prod. 2009;17(7):668-75.

[11] Meyer C. The greening of the concrete industry. Cem Concr Compos. 2009;31(8):601-5.

[12] Pasupathy K, Berndt M, Castel A, Sanjayan J, Pathmanathan R. Carbonation of a blended slag-fly ash geopolymer concrete in field conditions after 8 years. Constr Build Mater. 2016;125:661-9.

[13] Mohajerani A, Suter D, Jeffrey-Bailey T, Song T, Arulrajah A, Horpibulsuk S, et al. Recycling waste materials in geopolymer concrete. Clean Technol Environ Policy. 2019;21(3):493-515.

[14] Sanjuán MÁ, Estévez E, Argiz C, del Barrio D. Effect of curing time on granulated blast-furnace slag cement mortars carbonation. Cem Concr Compos. 2018;90:257-65.

[15] Meddah MS, Ismail MA, El-Gamal S, Fitriani H. Performances evaluation of binary concrete designed with silica fume and metakaolin. Constr Build Mater. 2018;166:400-12.

[16] Bucher R, Diederich P, Escadeillas G, Cyr M. Service life of metakaolin-based concrete exposed to carbonation: Comparison with blended cement containing fly ash, blast furnace slag and limestone filler. Cem Concr Res. 2017;99:18-29.

[17] Rath B, Debnath R, Paul A, Velusamy P, Balamoorthy D. Performance of natural rubber latex on calcined clay-based glass fiber-reinforced geopolymer concrete. Asian journal of Civil Engineering, 2020; 21: 1051-66.

[18] Haselbach L. Potential for carbon dioxide absorption in concrete. J Environ Eng. 2009;135(6):465-72.

[19] S M, TR P, M. Al-Mohaimeed A, Brindhadevi K, Pugazhendhi A. Characterization of polyurethane coating on high performance concrete reinforced with chemically treated Ananas erectifolius fiber. Prog Org Coatings [Internet]. 2021;150(July 2020):105977. Available from: https://doi.org/10.1016/j.porgcoat.2020.105977

[20] Rath B, Deo S, Ramtekkar G. A Proposed Mix Design of Concrete with Supplementary Cementitious Materials by Packing Density Method. Iran J Sci Technol Trans Civ Eng. 2020;1-15.

[21] Rath B, Deo S, Ramtekkar G. Modification of ACI209R-92 Concrete Shrinkage Model for Partial Replacement of Cement with Fly Ash and Sand with Pond Ash. Adv Civ Eng Mater. 2020;9(1):20200036.

[22] Berger RL, Young JF, Leung K. Acceleration of hydration of calcium silicates by carbon dioxide treatment. Nat Phys Sci. 1972;240(97):16-8.

[23] Monkman S, Shao Y. Carbonation curing of slag-cement concrete for binding CO 2 and improving performance. J Mater Civ Eng. 2010;22(4):296-304.

[24] Garrabrants AC, Kosson DS, DeLapp R, Kariher P, Seignette P, Van der Sloot HA, et al. Interlaboratory validation of the leaching environmental assessment framework (LEAF) method 1314 and method 1315. US Environ Prot Agency, Off Res Dev Res Triangle Park NC. 2012.

[25] EN BS. Concrete–Specification, performance, production and conformity. 2013.

[26] Malešič J, Kadivec M, Kunaver M, Skalar T, Cigić IK. Nano calcium carbonate versus nano calcium hydroxide in alcohols as a deacidification medium for lignocellulosic paper. Herit Sci. 2019;7(1):50.

[27] Garçon N, Friede M. Evolution of adjuvants across the centuries. In: Plotkin's Vaccines. Elsevier; 2018. p. 61-74.

[28] Kong DLY, Sanjayan JG. Effect of elevated temperatures on geopolymer paste, mortar and concrete. Cem Concr Res. 2010;40(2):334-9.

[29] Rashad AM. Potential use of phosphogypsum in alkali-activated fly ash under the effects of elevated temperatures and thermal shock cycles. J Clean Prod. 2015;87:717-25.

[30] Abdulkareem OA, Al Bakri AMM, Kamarudin H, Nizar IK, Ala'eddin AS. Effects of elevated temperatures on the thermal behavior and mechanical performance of fly ash geopolymer paste, mortar and lightweight concrete. Constr Build Mater. 2014;50:377-87.

[31] Kottititum B, Phung QT, Maes N, Prakaypan W, Srinophakun T. Early age carbonation of fiber-cement composites under real processing conditions: A parametric investigation. Appl Sci. 2018;8(2).

[32] Du X, Wang Y, Su X, Li J. Influences of pH value on the microstructure and phase transformation of aluminum hydroxide. Powder Technol. 2009;192(1):40-6.

[33] Pade C, Guimaraes M. The CO2 uptake of concrete in a 100 year perspective. Cem Concr Res. 2007;37(9):1348-56.

[34] Dunster AM, Bigland DJ, Holton IR. Rates of carbonation and reinforcement corrosion in high alumina cement concrete. Mag Concr Res. 2000;52(6):433-41.

[35] Salvoldi BG, Beushausen H, Alexander MG. Oxygen permeability of concrete and its relation to carbonation. Constr Build Mater. 2015;85:30-7.

[36] Talukdar S, Banthia N, Grace JR. Carbonation in concrete infrastructure in the context of global climate change–Part 1: Experimental results and model development. Cem Concr Compos. 2012;34(8):924-30.

[37] Yang K-H, Seo E-A, Tae S-H. Carbonation and CO2 uptake of concrete. Environ Impact Assess Rev. 2014;46:43-52.

[38] Ta V-L, Bonnet S, Kiesse TS, Ventura A. A new meta-model to calculate carbonation front depth within concrete structures. Constr Build Mater. 2016;129:172-81.

[39] Papadakis VG, Vayenas CG, Fardis MN. Fundamental Modeling and Experimental lnvestigation of. ACI Mater J. 1991;88(4).